

High-Power Laser-Mirror Faceplate Materials: Figures of Merit for Optical Distortion

Claude A. Klein

c.a.k. analytics, inc.

9 Churchill Lane, Lexington, MA 02173

105325.1146@compuserve.com

Abstract. High-power/high-energy (HEL) systems include an optical train consisting of mirrors and windows, which must be capable of transporting and directing the beam without seriously degrading the nominal performance of the laser. Since catastrophic failure modes are not a major threat at beam-power levels of current interest, the system's performance as measured in terms of achievable target irradiances can degrade as a result of thermal lensing, that is, the wavefront distortion caused by thermally induced phase aberrations. The purpose of this paper is to present an analytical investigation that addresses the problem of evaluating the impact of laser-driven mirror distortions; in this context it is shown how to obtain simple figures of merit (FoM) for rating the thermal lensing performance of mirror-faceplate material candidates. The performance of cooled HEL mirrors reflects their ability to minimize irradiance-mapping wavefront distortions, which leads to defining a thermal distortion coefficient $\xi = \alpha(1+\nu)$ that controls the out-of-plane growth of the faceplate. It is then straightforward to derive equations for characterizing the RMSsed surface deformation and to assess the merits of mirror-faceplate material candidates in a pulsed or a CW environment. Figures of merit for CW operation must take into account the requirement that the faceplate should be as thin as possible but still able to minimize coolant-induced pressure ripples; the modulus of elasticity, therefore, must be properly factored into FoM expressions. Since water-cooled HEL mirror heat-exchangers exhibit relatively modest Biot numbers ($Bi < 1$), the thermal conductivity of the faceplate is not a critical material parameter. Numerical evaluations demonstrate that the ranking of faceplate-material candidates does not depend on the laser mode of operation or the efficiency of the heat exchanger: It is the thermal expansion coefficient α that determines the performance if optical distortions are of concern. For this reason, diamond shows much promise, which will attract attention as CVD-diamond fabrication technologies mature.

Keywords. Figure of merit, heat exchanger, HEL system, high-power laser, material candidate, mirror faceplate, optical distortion, phase aberration, thermal lensing.

1. Introduction

The development of high-energy laser (HEL) systems for industrial and military purposes has stimulated a great deal of activity relating to the physics and the technology of optical components designed for handling powerful beams of coherent light. The reason for this is that typical HEL systems involve an optical train consisting of mirrors and windows, which must be capable of transporting and directing the beam without seriously degrading the nominal performance of the laser. Available experience indicates that, in general, catastrophic failure modes associated with thermally generated stresses or laser-induced damage are not a major threat at beam-power levels of current interest. The performance of the system as measured in terms of achievable target irradiances usually degrades because of “thermal lensing,” that is, the process of beam defocusing and beam distortion caused by thermally generated phase aberrations [1]. Since the operation of HEL systems requires close-to-diffraction-limited characteristics at the far-field focus, this lensing process must be carefully assessed and evaluated in relation to specific features of the optical train. In this paper I am presenting analytical investigations that address the issue of how laser-driven mirror-induced lensing impacts the performance of HEL systems; in this context I will derive simple expressions—called figures of merit (FoM)—for rating the ability of mirror-faceplate material candidates to minimize the distortion.

As demonstrated elsewhere [2], the performance of candidate materials for mirror faceplates or laser windows is best characterized by examining how wavefront distortions resulting from beam-generated thermal loadings affect the far field. If the distortions are axially symmetric and do not involve birefringence effects, the far-field intensity derives from the Huygens-Fresnel integral [3] and is given by the expression

$$I_{GF}(t) = \left(\frac{2\pi/\lambda}{Z_o} \right)^2 \left| \int_0^{D/2} \sqrt{I(r)} \exp[i\delta\phi(r,t)] r dr \right|^2 \quad (1)$$

in a cylindrical geometry.¹ The phase-aberration function $\delta\phi(r,t)$ maps the cumulative aberrations impressed on the beam while propagating through the system and relates to the optical path difference simply through the propagation constant $2\pi/\lambda$. In the absence of aberrations, that is, at the onset of thermal loadings ($t = 0$), the beam intensity at the Gaussian focus is

$$I_{GF}(0) = \text{BPF} \frac{\pi(D/2)^2 P}{(\lambda Z_o)^2}, \quad (2)$$

where BPF stands for the beam-profile factor that accounts for the reduction in far-field intensity caused by non-uniform beam intensities. As near-field phase aberrations emerge, the degradation in focal intensity obeys a Strehl-relation type equation [4],

$$I_{GF}(t) = I_{GF}(0) \times \text{SR} \quad (3)$$

with

$$\text{SR} = 1 - \text{var}[\delta\phi(r,t)] = 1 - (2\pi/\lambda)^2 \text{var}[\text{OPD}], \quad (4)$$

¹The notations are as specified in the Appendix.

which says that the optical train will remain nearly diffraction limited as long as the square root of the OPD variance does not exceed $\lambda/14$. The variance is defined as follows:

$$\text{var}[X] = \langle X^2 \rangle - \langle X \rangle^2, \quad (5)$$

the brackets symbolizing amplitude-weighted averages over the entire aperture, i.e.,

$$\langle X^n \rangle = \frac{\int_0^1 X^n \sqrt{I(\rho)} \rho d\rho}{\int_0^1 \sqrt{I(\rho)} \rho d\rho}. \quad (6)$$

Equation (4) provides an effective tool for evaluating the loss in focal irradiance caused by beam-induced phase aberrations. Throughout this paper I am relying on suitable expressions for the magnitude of $\sqrt{\text{var}[\text{OPD}]}$ to identify material properties or material property combinations that control the optical distortion and, thus, to derive proper figures of merit. In this manner I can address the problem coherently and formulate relatively straightforward but conceptionally correct equations for predicting the degradation in focal intensity and, by the same token, for rating the performance of HEL mirror-material candidates.

The selection of mirror-faceplate materials involves a variety of considerations and tradeoffs with regard to optical, thermal, and mechanical properties [5]. In Sec. 2 it is shown how a simple mirror model leads to the concept of a thermal distortion coefficient, ξ , which controls the magnitude of irradiance-mapping aberrations in a pulsed as well as in a continuous wave (CW) environment. The figure of merit that applies under pulsed conditions, that is, prior to the onset of significant heat transport across the faceplate then depends only on the heat capacity in addition to the distortion coefficient ξ (Sec. 3). Furthermore, in a CW regime and in the absence of coolant-induced pressure ripples, it becomes straightforward to obtain equations for characterizing the performance of actively cooled HEL reflectors and to assess the merits of mirror-faceplate materials under two limiting sets of conditions as specified by the efficiency of the heat-exchanger; figures of merit for the steady-state regime thus emerge in a direct manner (Sec. 4). In Sec. 5 I discuss performance ratings based on available data for faceplate-material candidates of current interest. The conclusions are stated in Sec. 6, and the symbols are identified in the Appendix.

2. Thermal Distortion Coefficient

Figure 1 illustrates the design concept currently implemented for manufacturing actively cooled high-power laser-light reflectors [5]. The mirror faceplate is typically 1-mm thick and is subjected to thermal loadings resulting from the unavoidable fractional absorption of incident radiation. Heat that is deposited at the front surface must be efficiently removed to prevent potentially damaging thermal stresses; this is the function of the heat-exchanger with its array of cooling channels immediately behind the faceplate, which is mounted on a backup structure designed to provide a stable, highly rigid base for the entire assembly. Because of the finite thermal conductivity of the faceplate material, there will be temperature gradients: Radial gradients that deform the front surface, and axial gradients that may alter the mirror curvature. Thermally induced surface deformations resulting from spatial variations in beam intensity generate “irradiance-mapping” wavefront distortions [6] that

impact the system's performance through the RMSsed OPD (see Sec. 1), which is

$$\sqrt{\text{var}[\text{OPD}]} = \frac{2}{\cos(\vartheta)} \sqrt{\text{var}[\delta l(\rho)]} \quad (7)$$

at an angle of incidence ϑ if $\delta l(\rho)$ refers to the out-of-plane growth of the mirror front surface for axisymmetric loadings. Mirror bowing involves low-spatial-frequency deformations that may give rise to first-order aberrations but "tend to be of second order for well designed mirrors" [5]; since they can be compensated by means of refocusing, I am postulating that mirror bowing can be ignored in the context of assessing the thermal lensing performance of HEL reflectors.

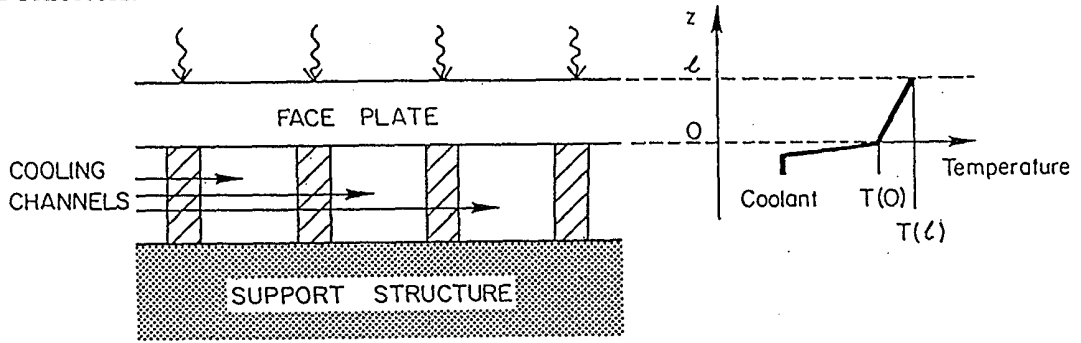


FIG. 1. Model configuration for evaluating thermally induced distortions of actively cooled high-power laser-beam reflectors. Faceplate and heat-exchanger are mounted on a rigid support structure that maintains the mirror back face in the $z = 0$ plane; mirror "bowing" is not a relevant factor. The temperature profile reflects situations occurring under steady-state conditions.

In this light, and for the purpose of investigating how the properties of the faceplate substrate material affect the thermal lensing process, we may consider the "simple mirror model" of Sparks as originally formulated in 1977 [7]. Approximations and assumptions are clearly stated and shown to provide an effective "Ansatz" for handling problems concerned with optical distortion or mechanical failure in high-power reflectors. With regard to issues of relevance here, this model postulates that:

- (a) Radial heat diffusion can be neglected, which implies that the thickness l of the faceplate must be small relative to the scale of spatial variations in beam intensity.
- (b) The back of the faceplate interfaces with the coolant fluid to ensure an adequate level of heat transfer but can be maintained in its original plane ($z = 0$).
- (c) Out-of-plane growth of the mirror front surface occurs only as a result of beam impingement and maps the incident irradiance pattern.

In this framework, it is the expansion of the faceplate caused by temperature increments $\delta T(\rho, z)$ that gives rise to out-of-plane growth of the front surface. This growth amounts to

$$\delta l(\rho) = \int_0^l \epsilon_z(\rho, z) dz \quad (8)$$

if $\epsilon_z(\rho, z)$ is the differential strain for axial expansion and includes stress-related contributions in accord with Hooke's law [8]. For axisymmetric loadings of elastically isotropic plates we

have

$$\epsilon_z(\rho, z) = \alpha\delta T(\rho, z) + (1/E) \{ \sigma_z(\rho, z) - \nu [\sigma_\rho(\rho, z) + \sigma_\theta(\rho, z)] \}, \quad (9)$$

the sigmas referring to the principal stress components. Thermally induced stresses are difficult to evaluate in a situation as applies here, with temperature distributions that depend on both axial and radial coordinates. For thin mirror faceplates ($l/D \ll 1$), however, plane-stress theory holds, which says that the faceplate will not be subjected to axial stresses; in other words, setting σ_z equal to zero should be a good approximation. Since the planar stresses are [9]

$$\sigma_\rho(\rho, z) = \alpha E \left[\int_0^1 \delta T(\rho', z) \rho' d\rho' - \frac{1}{\rho^2} \int_0^\rho \delta T(\rho', z) \rho' d\rho' \right] \quad (10)$$

$$\sigma_\theta(\rho, z) = \alpha E \left[\int_0^1 \delta T(\rho', z) \rho' d\rho' + \frac{1}{\rho^2} \int_0^\rho \delta T(\rho', z) \rho' d\rho' - \delta T(\rho, z) \right], \quad (11)$$

it follows that the axial strain is simply

$$\epsilon_z(\rho, z) = \alpha(1 + \nu)\delta T(\rho, z) - 2\alpha\nu \int_0^1 \delta T(\rho', z) \rho' d\rho'. \quad (12)$$

Returning now to Eq. (8), it is seen that the out-of-plane growth obeys the equation

$$\delta l(\rho) = \alpha(1 + \nu) \int_0^l \delta T(\rho, z) dz + \rho\text{-independent terms} \quad (13)$$

that do not contribute to the variance. This equation suggests to make use of a thermal distortion coefficient

$$\boxed{\xi = \alpha(1 + \nu)} \quad (14)$$

to denote the stress-augmented expansion of the mirror faceplate. In terms of figures of merit, this coefficient ξ plays the same role as the optical distortion coefficient χ of HEL windows [10].

3. Pre-Diffusion Regime

The nominal thermal diffusion time of a mirror faceplate of thickness l is [11]

$$\tau \simeq \frac{1}{\pi^2} \cdot \frac{l^2}{\kappa} \quad (15)$$

if κ represents the thermal diffusivity of the faceplate material.² Assume now that a short ($t \leq \tau$) pulse of laser light impinges on the mirror front surface. The deposited beam fluence generates a temperature increment $\delta T(\rho, z, t)$ that obeys the differential equation

$$A_M I(\rho, t) = \frac{d}{dt} \left[C_p' \int_0^l \delta T(\rho, z, t) dz \right] \quad (16)$$

²For a 1-mm thick molybdenum faceplate having a diffusivity of 0.55 cm²/s the thermal diffusion time τ is of the order of 2 ms.

where A_M stands for the mirror absorbance, and C'_p is the heat capacity (specific heat per unit volume) of the faceplate. For time-independent beam intensities Eq. (16) yields

$$A_M I(\rho) t = C'_p \int_0^l \delta T(\rho, z, t) dz, \quad (17)$$

which immediately tells us [see Eq. (13)] that prior to the onset of significant heat transport across the back surface, the front-surface deformation can be expressed as follows:

$$\delta l(\rho) = \xi A_M I(\rho) t / C'_p + \rho\text{-independent terms.} \quad (18)$$

This means that for pulses of duration t_0 we have

$$\sqrt{\text{var}[\delta l(\rho)]} = \frac{|\xi| A_M t_0}{C'_p} \sqrt{\text{var}[I(\rho)]}, \quad (19)$$

which identifies the parameters that impact the thermal lensing performance of the mirror. Note that the factor $|\xi| A_M t_0 / C'_p$ is in units of cubic centimeter per Watt and, thus, measures the optically significant growth of the mirror surface per unit incident power density. Furthermore, since multi-layer coatings are usually required to enhance the reflectivity of high-power laser mirrors, it is the coating that determines the magnitude of the absorbance A_M . In this light, and keeping in mind that the coating does not add much to the heat capacity [1], we conclude that the performance of the mirror with regard to minimizing the distortion in the pre-diffusion regime involves two substrate material parameters, ξ and C'_p , which combine into a figure of merit

$$\boxed{\text{FoM}_{pd} = \frac{C'_p}{|\xi|}} \quad (20)$$

that should be applicable under pulsed conditions. Evidently, this figure of merit also applies when the back surface is thermally insulated (adiabatic regime), in other words, in the absence of any effective cooling.

4. Steady-State Regime

The sudden onset of exposure to laser light causes transient (time-dependent) effects followed, at times $t \gg \tau$, by a thermal equilibrium situation defined as steady state. There is a constant flow of heat, $A_M I(\rho)$, across the back surface, which gives rise to a linear temperature gradient across the mirror faceplate (see Fig. 1). This gradient reflects the thermal conductivity of the substrate material and is described by the equation [11]

$$T(\rho, z) - T(\rho, 0) = \frac{A_M I(\rho)}{k} z, \quad (21)$$

where $T(\rho, 0)$ refers to the local temperature at the back surface. In equilibrium, and measured against the coolant, this temperature amounts to

$$T(\rho, 0) = \frac{A_M I(\rho)}{h} \quad (22)$$

if h represents the net effective heat-transfer coefficient to the coolant. Steady-state laser irradiation of the mirror faceplate thus results in temperature increments that can be described as follows:

$$\delta T(\rho, z) = A_M I(\rho) \times \left(\frac{1}{h} + \frac{z}{k} \right). \quad (23)$$

The axial temperature distribution originates from a temperature gradient across the mirror faceplate, which is controlled by the thermal conductivity k , and a temperature drop across the boundary layer, which is controlled by the heat-transfer coefficient h .

At this point, and in accord with Eq. (13), a simple integration yields

$$\delta l(\rho) = \xi \left(\frac{l}{h} + \frac{l^2}{2k} \right) A_M I(\rho) + \rho\text{-independent terms}, \quad (24)$$

which confirms that the faceplate surface deformation images, or maps, the beam “footprint.” If we introduce the Biot number,

$$Bi \equiv lh/k, \quad (25)$$

to characterize the efficiency of the heat-exchanger, it follows that the RMSsed surface deformation can be expressed in a manner such as

$$\sqrt{\text{var}[\delta l(\rho)]} = \frac{|\xi|l}{h} \left(1 + \frac{Bi}{2} \right) A_M \sqrt{\text{var}[I(\rho)]} \quad (26)$$

that best specifies how the performance of the mirror assembly depends on material properties and design features. Specifically, since the heat-transfer coefficient depends primarily on the coolant pressure and pathlength, it is immediately apparent that the faceplate should be as thin as possible but not thinner than required to minimize coolant-induced pressure ripples.

In terms of the figure of merit, this points to the modulus of elasticity (E) as an important faceplate-material property to consider [12]. In effect, since pressure-induced deflections (w) are essentially linear functions of the inverse flexural rigidity (FR), in other words, since the relation $w \propto 1/\text{FR}$, where

$$\text{FR} = \frac{El^3}{12(1-\nu^2)}, \quad (27)$$

normally applies [13], it follows that the recommended faceplate thickness relates to the allowable deflection in a manner such as

$$l_{\min}^3 \propto \frac{12(1-\nu^2)}{Ew_{\lim}}. \quad (28)$$

If E' is set equal to $E/(1-\nu^2)$, the figure of merit that emerges from Eq. (26) is therefore

$$\boxed{(\text{FoM})_{ss} = \begin{cases} \frac{\sqrt[3]{E'}}{|\xi|} & \text{if } Bi \ll 1 \\ \frac{\sqrt[3]{E'^2 k}}{|\xi|} & \text{if } Bi \gg 1 \end{cases}} \quad (29)$$

thus emphasizing that the cooling efficiency is another factor to consider. In principle, the thermal conductivity of the faceplate becomes significant only with highly efficient heat-exchangers. In this regard, we note that because of the complexities involved in augmenting the differential pressure per unit length of coolant flow [5], effective heat-transfer coefficients of more than $10 \text{ W}/(\text{cm}^2\text{K})$ may well be beyond the state of the art of water-cooled mirror technology. This implies Biot numbers of less than one under realistic conditions [$l \simeq 1 \text{ mm}$; $k \simeq 1 \text{ W}/(\text{cmK})$], which suggests that the thermal conductivity of the faceplate is actually irrelevant in the context of an FoM assessment of mirror-induced thermal lensing.³

5. Mirror Material Assessment

The FoM expressions formulated in Eqs. (20) and (29) provide a proper gauge for comparing the thermal lensing performance of mirror material candidates in a pulsed or a CW laser environment. To illustrate, we may consider the more promising materials listed in Table 1 of Anthony's [5] recent overview of high-heat-load optics — I added diamond in view of the remarkable potential of this material and much recent progress in CVD diamond technology — and take advantage of the comprehensive property data compilation published in Ref. 15. Note that the data I made use of refer to temperatures of 350 K and, hence, apply to normal laser operation; in this connection, it should be recognized that operation at cryogenic temperatures may involve very different property values (see, for instance, Fig. 5 of Ref. 5), which may affect the ratings in an unpredictable manner.

Ranking the candidates is best done on the basis of normalized figures of merit, or indices of merit defined as follows:

$$\text{IoM} = 100\left(\frac{\text{FoM}}{\text{FoM}_{\max}}\right), \quad (30)$$

where FoM_{\max} is the figure of merit of the candidate material best suited for the contemplated application. Figure 2 displays the results in the form of a grouped bargraph and demonstrates that mirror-faceplate materials can be ranked with regard to overall performance in the sense that if a material is superior in one application it is also superior in the others. The ranking (diamond→C/C→SiC→Si→Mo→Cu) essentially matches the inverse thermal distortion coefficient, which confirms that the thermal expansion of the mirror faceplate is the single most important factor to consider if beam distortions are of concern.

Specifically, Fig. 2 shows that:

- On a figure-of-merit basis, the two carbon materials, polycrystalline diamond and C/C composites, are both outstanding candidates, diamond exhibiting particular promise for high-heat-load optics applications that require efficient cooling, which has already attracted attention in the synchrotron community [16]. Carbon/carbon composites have been looked at in the early stages of HEL mirror development, but difficulties in adapting composite fabrication techniques to cooled mirror configurations led to the abandonment of this “approach” [5].

³Technologies based on porous media [14] show promise for achieving effective heat-transfer coefficients that exceed $50 \text{ W}/(\text{cm}^2\text{K})$, at which point the thermal conductivity may indeed become a significant mirror-material parameter.

- The two ceramics, silicon carbide and silicon, are the leading candidates for near-term HEL mirror development efforts, with Si providing the low-risk solution [17]. Still, it is anticipated that further progress in manufacturing CVD-SiC faceplates will lead to significantly improved performances and make this material the most cost-effective for suppressing irradiance-mapping distortions.
- For many years, molybdenum has been the high-power mirror “workhorse material” [5]; in addition to ease of machining and polishing, Mo exhibits a combination of physical properties that make it much more attractive than Cu (see Fig. 2), which was the first material used for cooled laser optics. Copper still plays an important role as a mirror material for industrial CO₂-lasers but cannot match the performance of the other popular substrate material (Si) when thermal lensing becomes an issue [18].

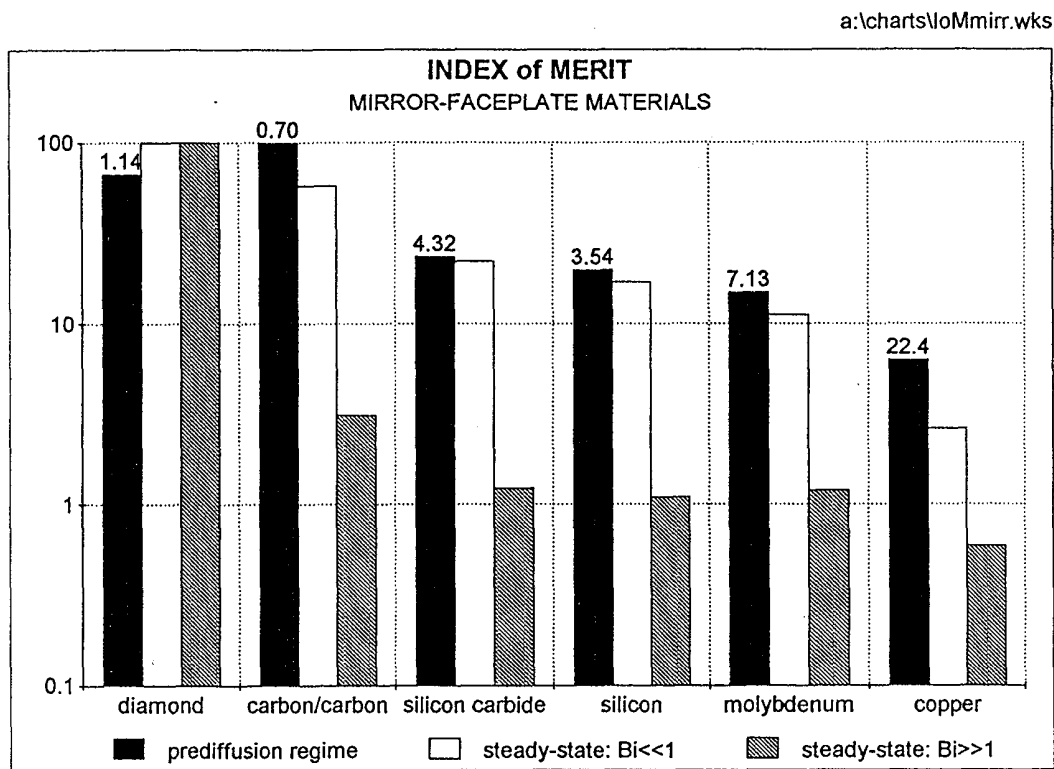


FIG. 2. Index of merit for thermal lensing of key mirror-faceplate materials. An index of 100 is assigned to the "best" candidate for each of the three operational regimes (Bi is the Biot number). The data labels are the values of the thermal distortion coefficient ξ in units of 10^{-6} K^{-1} .

6. Conclusion

This paper describes how issues relating to beam-induced wavefront distortions enter the material selection process for reflective HEL optics. Since the degradation in focal intensity is best expressed by means of a Strehl ratio [see Eq. (4)], the RMSsed OPD, or $\sqrt{\text{var}[\text{OPD}]}$ as defined in Sec. 1, provides an effective tool for developing guidelines in the context of assessing the thermal lensing performance of mirror-faceplate material candidates. These guidelines can be formulated in the form of figures of merit, but it must be recognized that there are no simple, universal criteria for rating the candidates; ultimately, even if mechanical failure is not an issue, the selection process involves considerations and tradeoffs that go beyond the requirement of driving the distortion coefficient ξ to zero.

Since the bowing of mirror faceplates can be compensated through refocusing, the thermal lensing performance of actively cooled HEL mirrors reflects their ability to minimize irradiance-mapping distortions. In this regard, the thermal distortion coefficient $\xi = \alpha(1+\nu)$ plays a key role in the sense that it controls the out-of-plane growth, δl , induced by the deposited beam fluence (short-pulse mode of operation) or the deposited beam intensity (CW mode of operation). The figures of merit for mirror-faceplate materials then emerge from the requirement to minimize the RMSsed surface deformation, $\sqrt{\text{var}[\delta l]}$, which yields the following expressions:

$$\begin{aligned} \text{for short-pulse operation:} & \quad C_p' / |\xi| \\ \text{for CW operation } (Bi \ll 1): & \quad \sqrt[3]{E' / |\xi|} \\ \text{for CW operation } (Bi \gg 1): & \quad \sqrt[3]{E'^2 k / |\xi|}. \end{aligned}$$

These figures of merit take into account the additional requirement that the faceplate should be as thin as possible but still able to prevent potentially significant coolant-induced pressure ripples. Note that, since state-of-the-art mirror heat-exchangers have relatively poor Biot numbers, the thermal conductivity is not a key material parameter.

Figure 2 demonstrates that the ranking of mirror-material candidates does not depend on the mode of operation or the efficiency of the heat-exchanger. It is the thermal expansion coefficient of the mirror faceplate that dominates the performance if optical distortions are of concern. For this reason, diamond shows exceptional promise, which undoubtedly will attract attention as CVD-diamond technologies mature. At this time, Si and SiC are the prime candidates, SiC exhibiting superior characteristics but still requiring further advances in fabrication methods.

Appendix: Nomenclature

A_M : mirror absorbance Bi : Biot number C_p' : heat capacity D : aperture diameter E : modulus of elasticity E' : modified elastic modulus h : heat-transfer coefficient I : beam intensity k : thermal conductivity l : faceplate thickness P : beam power r : radial coordinate t : elapsed time t_0 : pulse duration T : faceplate temperature w : coolant-induced deflection z : axial coordinate Z_0 : target range	α : thermal expansion coefficient ϵ : differential strain δl : out-of-plane growth $\delta\phi$: phase aberration δT : temperature increment ϑ : angle of incidence κ : thermal diffusivity λ : laser wavelength ν : Poisson's ratio ξ : thermal distortion coefficient ρ : reduced radial coordinate σ_x : principal stress component τ : thermal diffusion time BPF : beam-profile factor GF : Gaussian focus OPD : optical path difference SR : Strehl ratio
--	--

References

1. H. Bennett, "Thermal distortion thresholds for optical trains handling high pulse powers," in *Laser-Induced Damage in Optical Materials: 1976* (NBS Spec. Pub. 462, Washington, 1977), pp. 11-24.
2. C. Klein, "Thermally induced optical distortion in high-energy laser systems," *Opt. Eng.* **18**, 591-601 (1979).
3. M. Born and E. Wolf, *Principles of Optics: Fifth Edition*, Pergamon Press, Oxford (1975).
4. D. Holmes and P. Avizonis, "Approximate optical system model," *Appl. Opt.* **15**, 1075-1082 (1976).
5. F. Anthony, "High heat load optics: an historical overview," *Opt. Eng.* **34**, 313-320 (1995).
6. P. Avizonis, B. O'Neil, and V. Hedin, "Intensity mapping optical aberrations," *Appl. Opt.* **17**, 1527-1531 (1978).
7. M. Sparks, "Optical distortion and failure in high-power reflectors," in *Proc. High-Power Laser Optical Components Meeting: 1977* (Air Force Materials Lab., WPAFB/OH, 1978), pp. 66-80.
8. D. Mintzer, P. Tamarkin, and B. Lindsay, "Fundamental concepts of mechanics, units, and conversion factors," in *American Institute of Physics Handbook* (McGraw-Hill, New York, 1972), Sec. 2a.
9. B. Boley and J. Weiner, *Theory of Thermal Stresses*, J. Wiley, New York (1960).

10. C. Klein, "Optical distortion coefficients of high-power laser windows," *Opt. Eng.* **29**, 343-350 (1990).
11. H. Carslaw and J. Jaeger, *Conduction of Heat in Solids*, Oxford U. Press, Oxford (1959).
12. C. Klein, "Mirror figure of merit and material index of goodness for high-power laser-beam reflectors," *Proc. SPIE* **288**, 69-77 (1981).
13. S. Timoshenko and S. Woinowsky-Krieger, *Theory of Plates and Shells*, McGraw-Hill, New York (1959).
14. J. Rosenfeld and M. North, "Porous media heat exchanger for cooling of high-power optical components," *Opt. Eng.* **34**, 335-341 (1995).
15. C. Pellerin, F. Ayer, Y. Mehrotra, and A. Hopkins, "New opportunities from materials selection trade-offs for high precision space mirrors," *Proc. SPIE* **542**, 5-18 (1985).
16. A. Freund, "Diamond single crystals: the ultimate monochromator material for high-power x-ray beams," *Opt. Eng.* **34**, 432-440 (1995).
17. D. Seegmiller, private communication, W. J. Schafer Associates, Albuquerque (1996).
18. G. Herrit and H. Reedy, "Advanced figure of merit evaluation for CO₂ laser optics using finite element analysis," *Proc. SPIE* **1047**, 33-42 (1989).